γ-Glutamylcysteine Synthetase−Glutathione Synthetase: Domain Structure and Identification of Residues Important in Substrate and Glutathione Binding

Blythe E. Janowiak,‡ Michael A. Hayward, Francis C. Peterson, Brian F. Volkman, and Owen W. Griffith*

Department of Biochemistry, Medical College of Wisconsin, Milwaukee, Wisconsin 53226

Received December 5, 2005; Revised Manuscript Received July 10, 2006

ABSTRACT: In most organisms, glutathione (GSH) is synthesized by the sequential action of distinct enzymes, γ-glutamylcysteine synthetase (γ-GCS) and GSH synthetase (GS). In *Streptococcus agalactiae*, GSH synthesis is catalyzed by a single enzyme, γ-glutamylcysteine synthetase−glutathione synthetase (γ-GCS-GS). The N-terminal sequence of γ-GCS-GS is similar to *Escherichia coli* γ-GCS, but the C-terminal sequence is an ATP-grasp domain more similar to D-Ala, D-Ala ligase than to any known GS. In the present studies, C-terminally and N-terminally truncated constructs were characterized in order to define the limits of the γ-GCS and GS domains, respectively. Although WT γ-GCS-GS is nearly uninhibited by GSH ($K_i \sim 140$ mM), shorter γ-GCS domain constructs were unexpectedly found to be strongly inhibited ($K_i \sim 15$ mM), reproducing a physiologically important regulation seen in monofunctional γ-GCS enzymes. Because studies with *E. coli* γ-GCS implicate a flexible loop region in GSH binding, chimeras of *S. agalactiae* γ-GCS-GS were made containing γ-GCS domain flexible loop sequences from *Enterococcus faecalis* and *Pasteurella multocida* γ-GCS-GS, isoforms that are inhibited by GSH. Inhibition remained *S. agalactiae*-like (i.e., very weak). C-Terminal constructs of γ-GCS-GS have GS activity (0.01−0.04% of WT), but proper folding and significant GS activity required a covalently linked γ-GCS domain. In addition, site-directed mutants in the middle region of the γ-GCS-GS sequence established that GS activity depends on residues in a region that is also part of the γ-GCS domain. Our results provide new insights into the structure of γ-GCS-GS and suggest γ-GCS-GS evolved from a monomeric γ-GCS that became C-terminally fused to a multimeric ATP-grasp protein.

Glutathione (L-γ-glutamyl-L-cysteinylglycine, GSH)[1] is the main low molecular weight thiol in virtually all eukaryotes (*1*), in many Gram-negative bacteria (*2*, *3*), and in some Gram-positive bacteria (*3*, *4*). In eukaryotes and nearly all Gram-negative bacteria examined to date, GSH synthesis is catalyzed by the sequential action of two enzymes, γ-glutamylcysteine synthetase (γ-GCS) and GSH synthetase (GS). We recently reported that in *Streptococcus agalactiae*, a Gram-positive bacterium, GSH synthesis is catalyzed by a novel bifunctional GSH synthesis enzyme, which we named γ-glutamylcysteine synthetase−glutathione synthetase (γ-GCS-GS) (*5*). The enzyme is encoded by a single gene, *gshAB*, and catalyzes both the ATP-dependent ligation of glutamate and cysteine to form γ-glutamylcysteine (γ-GCS, reaction 1) and the ATP-dependent ligation of glycine to that intermediate (GS, reaction 2). Following our report, Y. Aharonowitz's group identified a similar enzyme, which they termed GshF, in another Gram-positive bacterium, *Listeria monocytogenes* (*6*), and J. Beeumen's group characterized the enzyme from *Pasteurella multocida*, a Gram-negative bacterium (*7*). Currently, gene sequences consistent with γ-GCS-GS proteins have been identified in 19 mostly Gram-positive bacteria (*5*−*7*), and it has been shown in *L. monocytogenes* that interruption of *gshAB* markedly increases bacterial sensitivity to oxidative stress and decreases survival in a mouse macrophage-like cell line (*6*). Because most of the bacteria having *gshAB* are human pathogens, we and others have suggested that γ-GCS-GS inhibitors may limit bacterial virulence and thus have utility as antibiotics (*5*, *6*). Understanding the structure, mechanism, and regulation of γ-GCS-GS is expected to facilitate the design of such compounds.

$$\text{L-glutamate} + \text{L-cysteine} + \text{ATP} \rightarrow \text{L-}\gamma\text{-glutamyl-L-cysteine} + \text{ADP} + P_i \quad (1)$$

$$\text{L-}\gamma\text{-glutamyl-L-cysteine} + \text{glycine} + \text{ATP} \rightarrow \text{GSH} + \text{ADP} + P_i \quad (2)$$

As reported previously, the N-terminal sequence of *S. agalactiae* γ-GCS-GS (amino acids 1−520) has significant homology with *Escherichia coli* γ-GCS (518 amino acids, 32% identity, 43% similarity), and the C-terminal sequence (amino acids 360−750) contains an ATP-grasp domain that is homologous to *E. coli* D-Ala, D-Ala ligase (24% identity, 38% similarity) (*5*). Notably, the regions homologous to *E. coli* γ-GCS and D-Ala, D-Ala ligase overlap by about 160

* To whom correspondence should be addressed. Tel: (414) 456-8778. Fax: (414) 456-6510. E-mail: griffith@mcw.edu.

‡ Present address: Department of Microbiology and Molecular Genetics, Harvard Medical School, Boston, MA.

[1] Abbreviations: GSH, glutathione; γ-GCS, γ-glutamylcysteine synthetase; GS, GSH synthetase; DTT, dithiothreitol; GSSG, glutathione disulfide; γ-GluCys, γ-glutamylcysteine; TEV, tobacco etch virus; WT, wild type; CD, circular dichroism; NMR, nuclear magnetic resonance; HSQC, heteronuclear single-quantum coherence; TROSY, transverse relaxation optimized spectroscopy.

10.1021/bi052483v CCC: $33.50
Published on Web 08/11/2006

amino acids. The present studies were designed to establish experimentally that the N-terminal and C-terminal regions account for the γ-GCS and GS activities of γ-GCS-GS, respectively, and to define the domain border. We find that the core γ-GCS domain is somewhat shorter than previously thought (residues 1−464) but that the GS domain apparently depends on residues in even that shorter sequence, being affected by a D448A site-directed mutation. Unexpectedly, we also found that some γ-GCS domain constructs were inhibited by GSH, a physiologically important feedback inhibitor of all monomeric γ-GCS enzymes but a molecule that has little effect on the activity of full-length *S. agalactiae* γ-GCS-GS. In contrast, GSH does inhibit the γ-GCS-GS of *Enterococcus faecalis* (present work) and *P. multocida* (*7*). We have explored the structural basis of this difference using chimeric enzymes and a homology-based model. Additional studies with GS domain constructs established that the proteins expressed well but had only very low GS activity. That result in combination with CD and NMR studies indicates that proper folding of the GS domain requires an intact γ-GCS domain.

EXPERIMENTAL PROCEDURES

Materials

Biochemical reagents were from Sigma unless indicated otherwise. Di-L-γ-glutamyl-L-cystine was synthesized from glutathione disulfide (GSSG) (*8*). Working solutions of L-γ-glutamyl-L-cysteine (γ-GluCys) were prepared by mixing the disulfide with 1 equiv of dithiothreitol (DTT). A modified pQE30 vector (Qiagen) that incorporates an N-terminal His_8 tag and a tobacco etch virus (TEV) protease cleavage site, pQE30T (*9*, *10*), was used for making expression plasmids. The His-tagged TEV protease was expressed and purified as described previously (*10*). Oligonucleotides were synthesized by Integrated DNA Technologies (Coralville, IA). [^{14}C]-Glycine was obtained from New England Nuclear. [^{15}N]Leucine and $^{15}NH_4Cl$ were obtained from Cambridge Isotope Laboratories.

Methods

Construction of Truncation Mutants of S. agalactiae γ-GCS-GS. The cloning of *S. agalactiae* γ-GCS-GS into an expression vector, pQE30T, was described previously (*5*). In the present studies, we used the intermediate cloning vector from that study, which consists of the entire *gshAB* gene flanked by ~100 bp of genomic sequence inserted into a TOPO cloning vector, pCR2.1 (BD Biosciences), as the template to clone the γ-GCS and GS domain constructs.

Five γ-GCS domain constructs were produced using in all cases an upstream primer, 5′ CGCGAGATCTCATGATTATCG 3′, that introduced a unique *Bgl*II restriction enzyme site (underlined) at the 5′ end and differing downstream primers that introduced a stop codon (bold) and an unique *Pst*I restriction enzyme site (underlined) at the residue of interest. The downstream γ-GCS domain primers were 5′ CGCGCTGCAG**TTA**TCCTTTTTGGATTACGTCAAATAGTAGC 3′, 5′ CGCGCTGCAG**TTA**AATATGCATATTGTGCC 3′, 5′ CGCGCTGCAG**TTA**TTCATCTAGGATTTTTTTTGTAA 3′, 5′ CGCGCTGCAG**TTA**TTTACGGTCAGTAAATTCATCTCC 3′, and 5′ CGCGCTGCAG**TA**ATCTTGGATTTGTGAAAAATAG 3′, for the constructs designated as GCS441Stop, GCS464Stop, GCS494Stop, GCS508Stop, and GCS520Stop, respectively.

Six GS domain constructs were produced using in all cases a downstream primer, 5′ CGCGCTGCAGCCTAGCCTAAGGAAC 3′, that introduced an unique *Pst*I restriction enzyme site (underlined) after the endogenous stop codon and differing upstream primers that introduced an unique *Bgl*II restriction enzyme site (underlined) at the residue of interest. The upstream GS domain primers were 5′ CGCGAGATCTATTACATATTTAGAAACTGTTCACC 3′, 5′ CGCGAGATCTCATTTTAACTTATCACG 3′, 5′ CGCGAGATCTATTGAGTACGTTAAAAATGGTAATATGA 3′, 5′ CGCGAGATCTATTGAGTACGTTAAAAATGGTAATATGA 3′, 5′ CGCGAGATCTGAAAAAGCATTTCCCAACTAA 3′, and 5′ CGCGAGATCTGATAAACCCGTCGTTAAGCC 3′ for the constructs designated as GSΔ293, GSΔ359, GSΔ440, GSΔ463, GSΔ493, and GSΔ519, respectively.

The amplified fragment for each of the 11 constructs was cut with *Bgl*II and *Pst*I restriction enzymes, and the fragment was introduced into the pQE30T expression vector (see Materials) immediately downstream of the His_8-TEV tag. All constructs were confirmed by DNA sequencing.

Construction of Site-Directed Mutants and Flexible Loop Chimeras of S. agalactiae γ-GCS-GS. Five mutant *S. agalactiae* γ-GCS-GS enzymes, H144A, D448A, K485A, K489A, and K526A, were made to examine the importance of single point mutations. Two chimeric mutants of *S. agalactiae* γ-GCS-GS were made to examine the role of a central flexible loop in the γ-GCS domain. All mutants were constructed by site-directed mutagenesis using Stratagene's QuikChange kit. The expression plasmid for WT *S. agalactiae* γ-GCS-GS (*5*) was used as the template, and the primers were designed per manufacturers' instructions, avoiding known rare codons for *E. coli*. Primers (mutated codon underlined) were as follows: H144A, 5′ CCATCTCTGGAATTGCCTATAATCTCGGTTTAGG 3′ and 5′ CCTAAACCGAGATTATAGGCAATTCCAGAGATGG 3′; D448A, 5′ CGAAGTGCTGGCGGAACAAGATCAATTCC 3′ and 5′ GGAATTGATCTTGTTCCGCCAGCACTTCG 3′; K485A, 5′ GCTATGGCTAACGCGGTTGTTACAAAAAAAATCC 3′ and 5′ GGATTTTTTTTGTAACAACCGCGTTAGCCATAGC 3′; K489A, 5′ GCTAACAAAGTTGTTACAGCGAAAATCCTAGATG 3′ and 5′ CATCTAGGATTTTCGCTGTAACAACTTTGTTAGC 3′; K526A, 5′ CCAATCGTCGTTGCGCCAAAATCTACAAACTTTGG 3′ and 5′ CCAAAGTTTGTAGATTTTGGCGCAACGACGATTGG 3′. The primers used to make the chimeric enzymes were (mutated bases underlined) 5′ CTAGAAAATGCTGTAGAAAACGGGCTGTTGAGCGAAGAGAAAGAATTTTAT 3′ and 5′ ATAAAATTCTTTCTCTTCGCTCAACAGCCCGTTTTCTACAGCATTTTCTAG 3′ for the changes needed to create the N-terminal region of the *E. faecalis* flexible loop, 5′ GAGAAAGAATTTTATGCACCTGTTCGTC 3′ and 5′ GACGAACAGGTGCATAAAATTCTTTCTC 3′ for the changes needed to create the C-terminal region of the *E. faecalis* loop, and 5′ CTAGAAAATGCTGTATCTACCGGGAAATTGATTGCTG 3′ and 5′ CAGCAATCAATTTCCCGGTAGATACAGCATTTTCTAG 3′ for the changes establishing a *P. multocida* flexible loop in *S. agalactiae* γ-GCS-GS. The sequences of all mutant constructs were confirmed by DNA sequencing.

Construction of the E. faecalis γ-GCS-GS Expression Plasmid. Genomic DNA from a sequenced strain of *E. faecalis*, 10C1 (NCIB 8661), was obtained from American Type Culture Collection (ATCC 11700). The putative γ-GCS-GS gene, *gshAB* [EF3089 (*11*)], was isolated from the genomic DNA using PCR to introduce *Bgl*II and *Hin*dIII restriction sites flanking the coding sequence. The primers used were (restriction enzyme sites underlined) 5′ CGCGAGATCTATGCACTCAAATCAATTATTACAGC-ATGC 3′ and 5′ CGCGAAGCTTTTATATCTTGGTGCTTA-TTTCAGGAAAGAGC 3′. The amplified product was cleaved by those restriction enzymes and inserted into the pQE30T expression vector (see Materials) immediately downstream of the His_8-TEV tag. The insert and flanking regions were sequenced to confirm that the vector insert matched that reported for EF3089 and coded for the native enzyme with an N-terminal His_8-TEV tag.

Expression and Purification of γ-GCS-GS Enzymes. E. faecalis γ-GCS-GS and mutant *S. agalactiae* γ-GCS-GS enzymes were expressed and purified as described for wild-type *S. agalactiae* γ-GCS-GS (*5*). Purified enzymes were stored in 20 mM HEPES, pH 7.8, containing 1 mM EDTA at 4 °C or were stored in aliquots at −80 °C in the same buffer to which glycerol was added to a concentration of 25%.

For 2D NMR experiments, *S. agalactiae* γ-GCS-GS, GCS464Stop, and GSΔ463 were labeled either uniformly with ^{15}N or with [^{15}N]leucine. To uniformly label the enzymes, they were expressed in SG13009 *E. coli* grown in M9 minimal medium containing 19 mM $^{15}NH_4Cl$ (*12*). To selectively label leucine residues, the enzymes were expressed in SG13009 *E. coli* in modified M9 media supplemented with 100 μg/mL concentrations of various amino acids and 100 μg/mL [^{15}N]leucine. Expression and purification of the ^{15}N-labeled enzymes relied on the same protocol as described previously (*5*) except that dialysis was against 8 L of 20 mM Tris-HCl buffer, pH 7.4, containing 5 mM $MgCl_2$. After dialysis overnight at 4 °C, the buffer in the enzyme sample was changed to 20 mM [$^2H_{11}$]Tris-HCl buffer, pH 7.4, containing 5 mM $MgCl_2$ by repeated concentration and dilution using a Centriprep centrifugal filter device (30 kDa M_r cutoff; Amicon-Millipore). Purified enzymes were stored in that buffer at 4 °C.

Cleavage of the His_8 Tag. A catalytic amount of His-tagged TEV protease (1:1000 mol/mol) was added to an aliquot of purified His-tagged enzyme, and the mixture was dialyzed against 8 L of appropriate buffer overnight at 4 °C. The His_6-TEV protease and the His_8 affinity tag were separated from the recombinant enzyme by incubation with 1 mL of Ni^{2+}-NTA resin. Washing the resin three times with 1 mL of 20 mM Tris-HCl buffer, pH 7.4, containing 5 mM $MgCl_2$ allowed collection of His_8-tag-free enzyme.

Analysis of Protein Concentration and Purity. Protein concentrations during purification were estimated by the method of Bradford (*13*). Final protein concentrations were determined on the basis of absorption at 280 nm using a molar absorption coefficient calculated on the basis of amino acid composition for each enzyme (*14*). Protein purity was determined by staining 10% SDS−PAGE gels with Coomassie Brilliant Blue and analyzing scans of the stained gels using LabImage version 2.7.1 (Kapelan Bio-Imaging). Molecular weight markers were obtained from Bio-Rad Laboratories.

Determination of the Quaternary Structure of S. agalactiae γ-GCS-GS and GCS464Stop. The M_r's of *S. agalactiae* γ-GCS-GS and GCS464Stop were estimated by FPLC using a Superdex 200 gel filtration column (1.65 × 85 cm; Amersham Biosciences) equilibrated and eluted with 50 mM MOPS buffer, pH 7.4, containing 5 mM $MgCl_2$ and 5 mM L-Glu. The proteins and other molecules used to produce the standard curve were as follows (M_r values): thyroglobin (670 kDa), bovine γ-globulin (158 kDa), chicken ovalbumin (44 kDa), equine myoglobin (17 kDa), and vitamin B_{12} (1.35 kDa) ("Gel Filtration Standards", Bio-Rad Laboratories). Standard and sample load volumes were 1 mL, and the flow rate was 1 mL/min. Fractions (1 mL) were monitored spectrophotometrically at 280 nm.

Assay of ADP Formation by γ-GCS or GS. To assay γ-GCS activity, substrate-dependent ADP formation was monitored using a pyruvate kinase- and lactate dehydrogenase-coupled assay as described previously (*5*). In brief, standard reaction mixtures (final volume 1.0 mL) contained 150 mM Tris-HCl buffer, pH 8.4, 0.2 mM EDTA, 100 mM KCl, 10 mM ATP, 40 mM $MgCl_2$, 100 mM L-glutamate, 10 mM L-cysteine, 10 mM phospho(enol)pyruvate, 0.42 mM NADH, 12.5 mM ammonium sulfate, 20 IU pyruvate kinase, and 30 IU lactate dehydrogenase. Reaction mixtures were equilibrated to 37 °C, and reaction was initiated by addition of enzyme. Background rates were determined in the absence of L-cysteine and subtracted. The rate of ADP formation was assumed to equal the rate of NADH oxidation as monitored at 340 nm ($\epsilon = 6.2\ mM^{-1}$). One unit of γ-GCS activity is the amount of enzyme forming 1 μmol of product/h.

Assay mixtures for determination of GS were similar to those used for γ-GCS except L-glutamate and L-cysteine were replaced by 25 mM γ-GluCys (generated in situ as described in Materials) and 25 mM glycine. Background rates were determined in the absence of γ-GluCys. One unit of GS is the amount of enzyme forming 1 μmol of product/h.

The K_m values of γ-GCS and GS substrates were determined using the ADP formation assays with varying substrate concentrations. Nonvaried substrates were present at concentrations above their K_m values (see table legends). Where it was of interest to compare activities of enzymes of different molecular weights (e.g., to compare domains to full-length γ-GCS-GS), specific activities were expressed as units per nanomole of enzyme, instead of the traditional units per milligram of enzyme.

Inhibition of γ-GCS Activity by GSH and γ-GluCys. To determine if inhibition was competitive vs L-glutamate, K_i values for GSH and γ-GluCys were determined using the ADP formation assay with reaction mixtures containing 1 mM L-cysteine (∼10-fold its K_m) and 5−100 mM L-glutamate. For shorter *S. agalactiae* γ-GCS-GS constructs and *E. faecalis* γ-GCS-GS (i.e., enzymes for which GSH is a good inhibitor), GSH was varied from 0 to 40 mM. For full-length *S. agalactiae* γ-GCS-GS and contructs that are poorly inhibited by GSH, GSH was varied from 0 to 200 mM. For inhibition by γ-GluCys for all enzymes, the inhibitor was varied from 0 to 20−40 mM. Studies with *E. coli* γ-GCS were carried out similarly except L-glutamate was varied from 0.5 to 10 mM.

Reconstitution of S. agalactiae γ-GCS-GS Using Paired Domain Constructs. To determine if activity of GS domains could be rescued by adding the missing γ-GCS domain, paired enzymes (i.e., GCS441Stop and GSΔ440, GCS464Stop and GSΔ463, GCS494Stop and GSΔ493, GCS520Stop and GSΔ519) were incubated together. Incubations were performed on ice for varying lengths of time (5 min to 2 h) in 20 mM HEPES buffer, pH 7.8, containing 1 mM EDTA. Enzymes were incubated in 1:1, 1:2, and 1:4 γ-GCS:GS molar ratios. After the incubations, both activities, γ-GCS and GS, were determined using the ADP formation assays described above.

Assay of [^{14}C]GSH Synthesis. To determine GSH formation by the GS activity of *S. agalactiae* γ-GCS-GS and the GS domains, the incorporation of [^{14}C]glycine into L-γ-glutamyl-L-cysteinyl[^{14}C]glycine (i.e., [^{14}C]GSH) was determined as described previously (*5*). Briefly, reaction mixtures contained, in a final volume of 0.4 mL, 150 mM Tris-HCl buffer, pH 8.4, 100 mM KCl, 40 mM $MgCl_2$, 0.3 mM EDTA, 10 mM ATP, 20 mM PEP, 50 mM γ-GluCys, 3 mM [^{14}C]glycine, 9 IU of pyruvate kinase, 2.5 mM ammonium sulfate, and 1 mM aminooxyacetic acid (to inhibit any contaminating transaminases). Reactions were initiated by addition of purified *S. agalactiae* γ-GCS-GS or GS domain, and portions (100 μL) were removed at specified time points and quenched by addition to ice-cold 20 mM acetic acid (1 mL). A 1 mL portion of those solutions was applied to a small column (0.5 × 8 cm) of Dowex 1 (acetate form), and the resin was then washed with 5 column volumes (10 mL) of 20 mM acetic acid to remove unreacted [^{14}C]-glycine. Product [^{14}C]GSH was then eluted with 1.5 mM ammonium acetate (4 mL) and quantitated by liquid scintillation counting.

Circular Dichroism (*CD*) *Experiments*. WT *S. agalactiae* γ-GCS-GS and *S. agalactiae* γ-GCS and GS domains, purified as described above, were dialyzed overnight at 4 °C against 16 L of 5 mM KP_i, pH 7.0, and then diluted to 10 μM in the same buffer immediately prior to analysis by CD. Spectra were obtained using a JASCO J-710 CD spectropolarimeter and a 1 mm cell path, taking an average of five scans from 200 to 250 nm, sampling every 0.1 nm.

Nuclear Magnetic Resonance (*NMR*) *Experiments*. ^{1}H 1D NMR and ^{1}H−^{15}N 2D heteronuclear single-quantum coherence (HSQC) (*15*) and transverse relaxation optimized spectroscopy (TROSY) (*16*) NMR spectra were acquired at 25 °C using a Bruker DRX 600 NMR spectrometer equipped with a ^{1}H/^{15}N/^{13}C TXI Cryoprobe. NMR samples contained 90% H_2O, 10% D_2O, and ∼0.5 mM enzyme in 20 mM [$^2H_{11}$]-Tris-HCl, pH 7.4, containing 5 mM $MgCl_2$.

Modeling of the γ-GCS Domain of S. agalactiae γ-GCS-GS. On the basis of the γ-GCS domain construct activity results, an alignment was made between the full-length *E. coli* γ-GCS (518 amino acids) and the 1−464 sequence of *S. agalactiae* γ-GCS-GS using T-Coffee version 2.03 (*17*). On the basis of that alignment and the *E. coli* γ-GCS crystal structure (PDB codes 1VAG and 1V46) (*18*), a homology-based model of the 1−464 *S. agalactiae* sequence was constructed using Modeller version 7.7 (*19*, *20*). Five models were generated using the default settings for simple homology-based modeling, and the model with the lowest objective function value, as determined by Modeller, was selected. The stereochemical quality of the selected model was then examined using several 3D model verification programs: PROCHECK (*21*), PROVE (*22*), ANOLEA (*23*), and ERRAT2 (*24*).

RESULTS

Characterization of the N-Terminal γ-GCS Domain of S. agalactiae γ-GCS-GS. As reported previously (*5*), the sequence of the N-terminal 520 amino acids of *S. agalactiae* γ-GCS is homologous to *E. coli* γ-GCS (518 amino acids), and many of the active site residues identified for *E. coli* γ-GCS (*18*, *25*) are conserved in *S. agalactiae* γ-GCS-GS (Figure 1A, top sequence). Notably, all of the amino acids known to be involved in substrate and metal ion binding occur prior to residue 283, and sequence similarity diminishes significantly but not completely beyond residue 294.

In *E. coli* γ-GCS the three C-terminal α-helices lie on the outer surface of the structure, relatively remote from the active site region (Figure 1B). We hypothesized that the corresponding sequences in *S. agalactiae* γ-GCS-GS might not be required for γ-GCS activity but might rather serve as a link or interface with the GS domain. To test this hypothesis, we expressed the longest plausible γ-GCS domain (residues 1−520) and four constructs in which the putative C-terminal flexible loop "tail" and three helices were sequentially deleted (residues 1−508, 1−494, 1−464, and 1−441). These proteins were designated GCS520Stop, GCS508Stop, GCS494Stop, GCS464Stop, and GCS441Stop, respectively.

All five γ-GCS domains expressed well and were purified to >95% homogeneity. As expected, the enzymes had no detectable GS activity, and all showed significant, albeit varied, γ-GCS activity (Table 1). Expressed on a units per nanomole protein basis, the shortest enzyme, GCS441Stop, was only 9% as active as WT *S. agalactiae* γ-GCS-GS. In contrast, GCS464Stop had 148% the activity of WT γ-GCS-GS, and longer constructs had progressively decreasing activity (95%, 51%, and 37% of WT activity for GCS494Stop, GCS508Stop, and GCS520Stop, respectively).

The expressed γ-GCS domains were also characterized with respect to substrate K_m values and compared to WT γ-GCS-GS (Table 1). As shown, K_m values for ATP are similar to WT γ-GCS-GS for all of the constructs, and the K_m values for L-cysteine are generally similar albeit modestly (67%) higher for GCS508Stop. In contrast, the K_m value for L-glutamate is ∼3-fold higher for GCS441Stop than for WT γ-GCS-GS and the other constructs.

Glutathione is a potent nonallosteric feedback inhibitor of all eukaryotic and prokaryotic monofunctional γ-GCS enzymes (*27*−*29*) but was found to be only a very weak inhibitor of the bifunctional γ-GCS-GS of *S. agalactiae* (K_i > 100 mM) (*5*). Interestingly, while the longest *S. agalactiae* γ-GCS constructs, GCS508Stop and GCS520Stop, like full-length γ-GCS-GS (*5*), are not significantly inhibited by GSH [K_i: 140−312 mM (Table 1)], the shorter *S. agalactiae* γ-GCS constructs, GCS464Stop and GCS494Stop, are strongly inhibited [K_i: 13 and 18 mM, respectively (Table 1)]. In all cases, inhibition was largely competitive with L-glutamate with some evidence of mixed inhibition.

Similar studies were carried out with γ-GluCys to determine if it was the glycine residue of GSH that prevented its binding to GCS508Stop, GCS520Stop, and WT γ-GCS-GS.

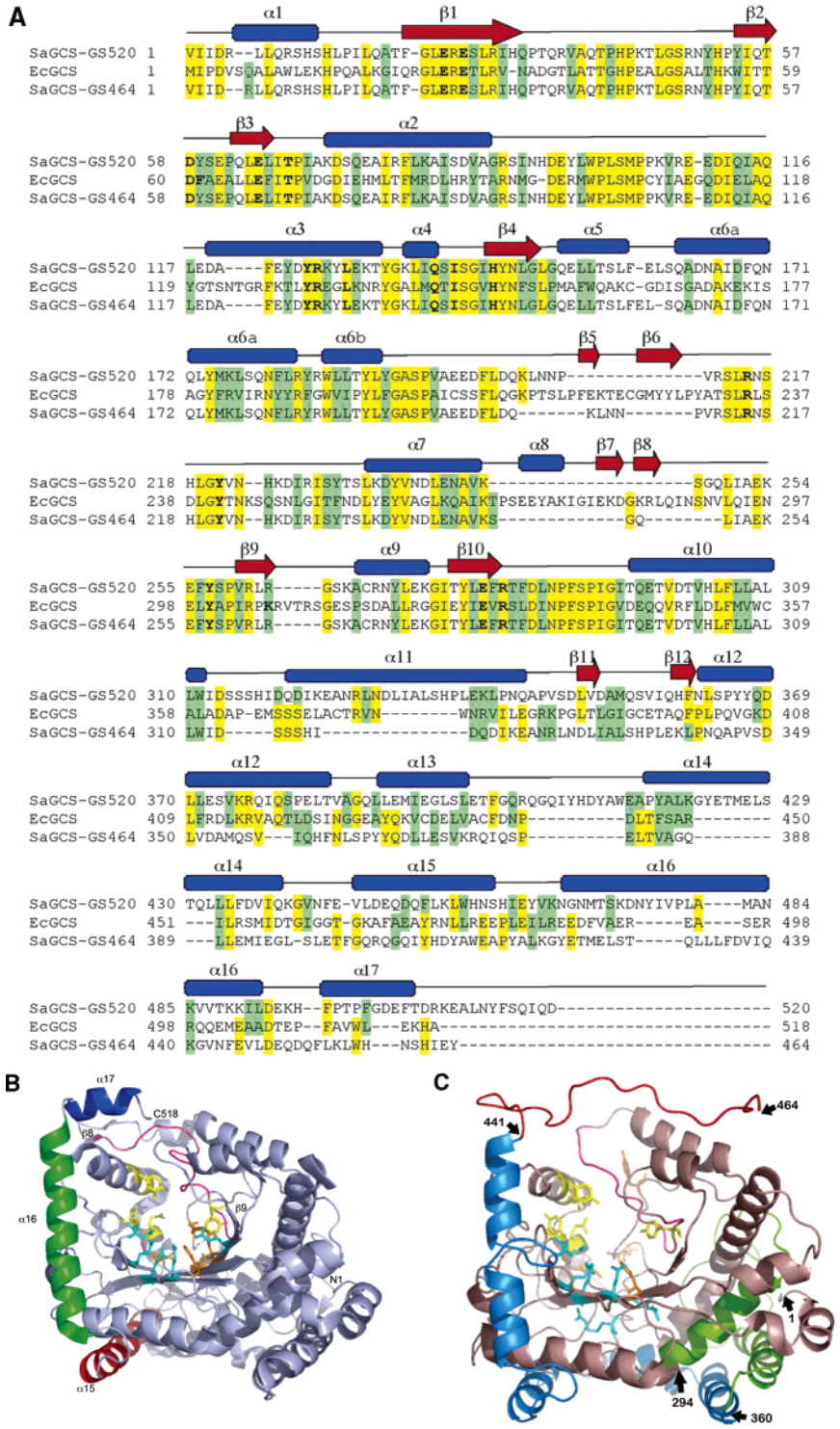

FIGURE 1: Alignment, models, and putative active site of the N-terminal domain of *S. agalactiae* γ-GCS-GS. Panel A: Alignments showing homology of the N-terminal sequence of *S. agalactiae* γ-GCS-GS with *E. coli* γ-GCS (EcGCS). The top and bottom lines show the alignment between *E. coli* γ-GCS and residues 1−520 and 1−464 of *S. agalactiae* γ-GCS-GS (SaGCS-GS520 and SaGCS-GS464, respectively). The top alignment was constructed using Clustal W (*26*), and the bottom alignment was made by using T-Coffee, version 2.03 (*17*). Yellow and green highlighted regions indicate residues that are identical and similar in the two sequences, respectively. Bold residues indicate putative key residues as identified in *E. coli* γ-GCS (*18*, *25*). *E. coli* γ-GCS secondary structure (*18*) is depicted by blue bars (α-helices) and red arrows (*β*-sheets) above the alignment. Panel B: Cartoon of *E. coli* γ-GCS in the open conformation (i.e., without substrates or inhibitors in the active site) based on its crystal structure (PDB code 1V4G) (*18*). Active site residues are shown as sticks (cyan = Mg^{2+}/ATP binding, orange = glutamate binding, and yellow = cysteine binding). The C-terminal α-helices that defined truncation points in the corresponding γ-GCS-GS γ-GCS domain model are labeled, and the central flexible loop between *β*-sheets 8 and 9 that is thought to play a role in GSH inhibition is colored pink. Panel C: Model of the N-terminal region (residues 1−464) of *S. agalactiae* γ-GCS-GS based on the crystal structure of *E. coli* γ-GCS in the closed conformation (PDB code 1VA6) and the bottom alignment shown in panel A. The proposed active site is shown using the same color scheme as in panel B. The points of truncation are marked and follow the same color scheme as the C-terminal α-helices shown in panel B. In addition, residues 294−359 are shown in chartruse and residues 360−440 are shown in aquamarine to point out regions that were used as points of truncation for the GS domains (i.e., N-terminal deletion constructs). The figures were made using MacPyMOL (DeLano Scientific, LLC).

Table 1: Comparison of K_m Values for γ-GCS Substrates, K_i Values for GSH and γ-GluCys Inhibition, and V_{max} Values for γ-GCS Activity among *S. agalactiae* γ-GCS Domains and WT γ-GCS-GS

kinetic constant[a]	GCS441Stop	GCS464Stop	GCS494Stop	GCS508Stop	GCS520Stop	WT γ-GCS-GS[d]
K_m (L-Glu) (mM)	77 ± 6	23 ± 0.9	22 ± 1.0	34.7 ± 1.3	28.9 ± 3.9	22 ± 1
K_m(L-Cys) (μM)	166 ± 3	138 ± 7	171 ± 7	260 ± 13	161 ± 2	156 ± 9
K_m(ATP) (μM)	65 ± 6	66 ± 2	65 ± 4	82 ± 16	60 ± 5	64 ± 11
K_i(GSH) (mM)	ND[c]	12.9 ± 0.6	18.2 ± 0.7	277 ± 48	312 ± 73	141 ± 23
K_i(γ-GluCys) (mM)	ND[c]	7.6 ± 0.3	24.3 ± 2.5	34 ± 8	13.7 ± 2.3	10.2 ± 1.2
V_{max} (units/nmol)[b]	9.4 ± 0.2	163 ± 0.4	104.2 ± 0.3	56.4 ± 2.9	40.4 ± 0.4	109.7 ± 0.5

[a] γ-GCS activity of γ-GCS-GS was assayed on the basis of ADP formation as described in Methods. Values shown are means ± SD for at least triplicate determinations. Saturating levels of nonvaried substrates were used: 100 mM L-glutamate, 10 mM L-cysteine, 10 mM ATP, and 35 mM $MgCl_2$. [b] V_{max} values shown are the means ± SD from all substrate studies. [c] ND, not determined. [d] Reference *5*.

Inhibition by γ-GluCys was uniformly strong [K_i: 8−34 mM (Table 1)].

Model of the N-Terminal γ-GCS Domain of S. agalactiae γ-GCS-GS. On the basis of the activity results, it is apparent that the 1−464 sequence most closely represents the true γ-GCS domain. Therefore, residues 1−464 were aligned with the full-length *E. coli* sequence (Figure 1A, bottom sequence).[2] A homology-based model of that alignment was constructed using the crystal structure of *E. coli* γ-GCS (Figure 1B) as the template. The resulting γ-GCS domain model (Figure 1C) was of higher quality, particularly as judged by PROCHECK, than an earlier model (not shown) based on an alignment using the full 1−520 sequence of *S. agalactiae* γ-GCS-GS. Importantly, both the overall active site geometry and all of the key active site residues identified for *E. coli* γ-GCS are preserved in the γ-GCS domain model with the sole exception of a Tyr for Phe substitution at residue 59 of *S. agalactiae* γ-GCS-GS (Figure 1A).

Model of the C-Terminal GS Domain of S. agalactiae γ-GCS-GS. As noted earlier, the C-terminal region (residues 360−750) of *S. agalactiae* γ-GCS-GS is weakly homologous to *E. coli* D-Ala, D-Ala ligase (*30*) and *E. coli* GS (*31*). Despite weak homology, we proposed that the C-terminal region is responsible for the GS activity observed (*5*). That view was confirmed for *L. monocytogenes* γ-GCS-GS by showing that truncation at residue 466 allowed continued in vivo formation of γ-GluCys but not GSH (*6*). The γ-GCS-GS domain border and properties of the truncated protein were, however, not established. Therefore, we developed a structure-based alignment of the C-terminal region of *S. agalactiae* γ-GCS-GS (residues 382−750) based on a consensus fold of *E. coli* GS and D-Ala, D-Ala ligase (*32*), both of which are ATP-grasp domain enzymes (not shown). Although the resulting alignment achieved 24% and 18% identity (38% and 33% similarity) with D-Ala, D-Ala ligase and GS, respectively, only 9 of the 26 residues proposed to be important for *E. coli* GS activity aligned in the *S. agalactiae* γ-GCS-GS sequence. As expected, specific alignments in the N-terminal part of the domain are highly dependent on where one views the GS domain as starting. Sequence homology alone suggests a start as early as residue 360 (*5*), our best structural alignment suggests a start at residue 382, and consideration of the γ-GCS domain activities suggests the GS domain starts after residue 464.

[2] While this paper was under review, B. Vergauwen et al. reported on the γ-GCS-GS from *P. multocida* and provided an alignment of the N-terminal γ-GCS domain that differs only slightly from that shown in Figure 1A, lower sequence. Differences are confined to the C-terminal region of the domain where homology to *E. coli* sequences is weak (*7*).

Table 2: Comparison of GS Specific Activity among *S. agalactiae* GS Domain Enzymes and WT γ-GCS-GS

enzyme	GS specific activity (units/nmol of enzyme)[a]	% WT GS activity
GSΔ293	0.00025 ± 0.00002	0.0012
GSΔ359	0.00034 ± 0.00001	0.0014
GSΔ440	0.0048 ± 0.0003	0.019
GSΔ463	0.0111 ± 0.0006	0.045
GSΔ493	0.0034 ± 0.0003	0.014
GSΔ519	0.0016 ± 0.0001	0.0063
γ-GCS-GS	25.1 ± 0.4	100

[a] GS specific activity was assayed on the basis of incorporation of [^{14}C]glycine into [^{14}C]GSH as described in Methods. Activity values shown are means ± SD for triplicate determinations. Note that specific activity of WT γ-GCS-GS corresponds to 285 units/mg, which is lower than seen with the standard assay because the [^{14}C]glycine concentration was held at about 10% K_m to increase sensitivity.

Very recently, B. Vergauwen et al. (*7*) proposed a GS domain alignment for both *P. multocida* and *S. agalactiae* γ-GCS-GS that is based on cynophycin synthases in addition to D-Ala, D-Ala ligases and, like our best model, begins at residue 381. Experimental support for the alignment or a structural model was not provided.

Characterization of S. agalactiae GS Domains. In the absence of unequivocal GS domain models, we designed C-terminal domain constructs based on the γ-GCS domain results and sequence homology. Thus, a construct was made starting at residue 294, the point at which significant γ-GCS homology declines, and another was made using the largest plausible GS homology region, residues 360−750 (*5*), since that also captured the 382−750 sequence implicated in our best structure-based alignment and the sequence-based alignment of B. Vergauwen et al. (*7*). In addition, domains were made that complemented each of four γ-GCS domain constructs, GCS441Stop, GCS464Stop, GCS494Stop, and GCS520Stop. The six GS domain constructs were designated GSΔ293, GSΔ359, GSΔ440, GSΔ463, GSΔ493, and GSΔ519, where Δ*XXX* indicates the number of N-terminal amino acids deleted from the WT γ-GCS-GS sequence (see Methods). All six GS domains were expressed as described in Methods, and all except the smallest (GSΔ519) were isolated in at least 75% purity. Despite several attempts, GSΔ519 could not be purified to yield a predominant band at the appropriate M_r on SDS−PAGE (data not shown). Attempts to further purify the other GS constructs on Superdex 200 resulted in substantial loses of protein without significant improvement in purity (data not shown).

As expected, the expressed putative GS domains had no detectable γ-GCS activity, but surprisingly, the proteins also exhibited very little GS activity. As shown in Table 2, GS activity ranged from 0.001% of WT in the longest expressed

domains (GSΔ293 and GSΔ359) to 0.045% of WT in GSΔ463, the GS domain corresponding to the deletion made in constructing the most active γ-GCS domain. In view of the uniformly low activities, K_m values for the substrates were not determined.

To eliminate the possibility that the N-terminal His_8 tag was interfering with the folding and/or activity of the GS domain constructs, the His_8 tag was removed using TEV protease, and the domains were repurified. Cleaved proteins were recovered in good yield, but GS activity was not improved (data not shown). In similar studies, treatment of full-length γ-GCS-GS with TEV protease caused no significant loss of activity or protein following purification as described in Methods (data not shown).

We considered the possibility that GS activity could be rescued by addition of the complementary γ-GCS domain enzyme. As detailed in Methods, paired expressed domains (e.g., GCS441Stop and GSΔ440) were incubated on ice and then assayed for both γ-GCS and GS activity. The γ-GCS activity was undiminished, and the GS activity remained essentially undetectable with the ADP formation assay used (i.e., <1% of WT; data not shown).

Evaluation of Domain Folding by Circular Dichroism (CD) Spectroscopy. To assess folding, CD spectra of WT γ-GCS-GS and of γ-GCS and GS domains (10 μM each) were compared. As shown in Figure 2A, two main negative peaks (at ~208 and ~222 nm) are visible in the spectra of the four γ-GCS domains tested and in the full-length γ-GCS-GS spectrum. These peaks suggest that the enzymes are well-folded and contain significant helical structure, consistent with the α-helix-rich γ-GCS domain model shown in Figure 1C.

In contrast, the shorter expressed GS domains (GSΔ440, GSΔ463, GSΔ493, and GSΔ519) exhibit weaker CD signals with virtually no distinct peaks in the spectra (Figure 2B). The results are consistent with unfolded or poorly folded structures. If it is assumed, on the basis of their good enzymatic activity and strong CD signals, that the expressed γ-GCS domains and full-length γ-GCS-GS are properly and equally well folded, then theoretical, albeit approximate, CD spectra for four of the GS domains can be calculated by subtracting the γ-GCS domain CD spectra from the γ-GCS-GS spectrum. As shown in Figure 2B, the observed GS CD spectra do not match the predicted spectra. The longest GS domain constructs, GSΔ293 and GSΔ359, show CD spectra that are of intermediate character, suggesting some secondary structure is present although the proteins are still without significant GS activity (Figure 2C).

Evaluation of Domain Folding by Nuclear Magnetic Resonance (NMR) Spectroscopy. We used ^1H 1D NMR and $^1H-^{15}N$ 2D (HSQC and TROSY) experiments to further characterize the folding of selected *S. agalactiae* γ-GCS and GS domains. Consistent with the presence of stable tertiary structure, the ^1H 1D NMR spectra of γ-GCS-GS and GCS464Stop contain signals in the amide region downfield of 10 ppm (Figure 3A). These peaks are more distinct in the spectrum of GCS464Stop than in γ-GCS-GS, an observation attributable to the significantly smaller size of GCS464Stop (monomer; M_r ~54000) vs γ-GCS-GS (dimer; total M_r ~176000). In contrast, there are no visible peaks in the same regions of the GSΔ463 spectrum despite its small size (subunit M_r ~32000; expected dimer of M_r ~64000). Spectra for GSΔ440 and GSΔ359 were indistinguishable from the GSΔ463 spectrum shown.

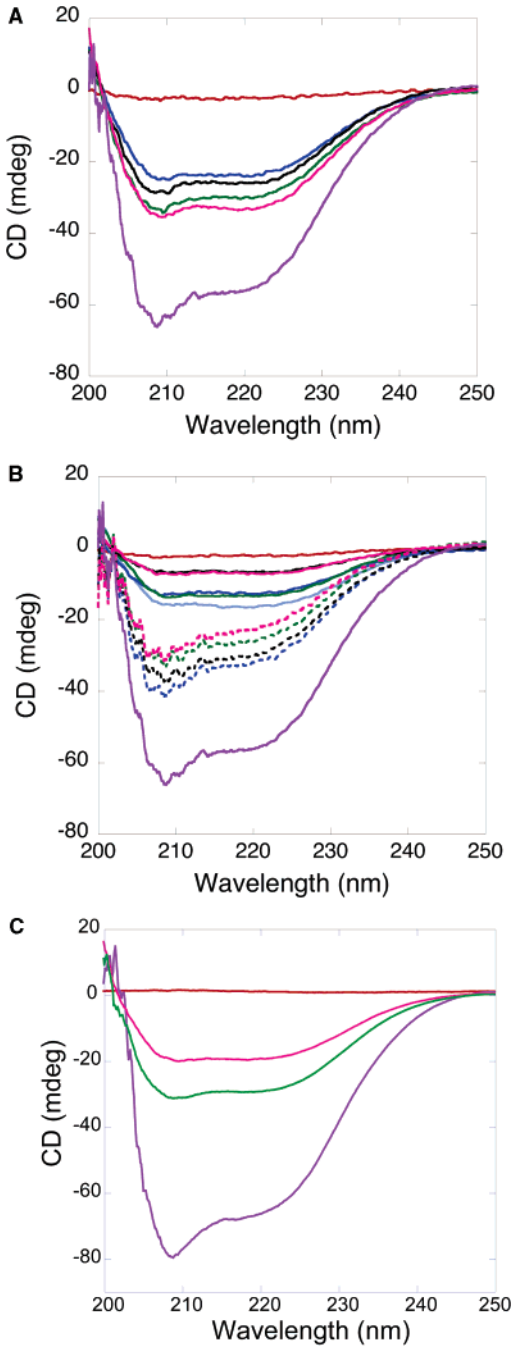

FIGURE 2: Circular dichroism (CD) spectra of expressed γ-GCS domains and GS domains. All enzymes were examined at 10 μM in 5 mM KP_i buffer, pH 7.0. In all panels the spectrum of buffer alone is shown in red. Panel A: Comparison of CD spectra of γ-GCS domains (GCS441Stop, blue; GCS464Stop, green; GCS-494Stop, black; GCS520Stop, pink) with WT *S. agalactiae* γ-GCS-GS (purple). Panel B: Comparison of CD spectra of the shorter GS domains (GSΔ440, blue; GSΔ463, green; GSΔ493, black; GSΔ519Stop, pink) with WT *S. agalactiae* γ-GCS-GS (purple). Theoretical GS CD spectra (dotted lines) were calculated by subtracting the γ-GCS domains' spectra (panel A) from the full-length enzyme spectrum as discussed in the text. Panel C: Comparison of CD spectra of the longest GS domains (GSΔ293, pink; GSΔ359, green) with WT *S. agalactiae* γ-GCS-GS (purple).

Because 1D NMR spectra are not always reliable indicators of folding in helical proteins, we also acquired $^1H-^{15}N$ 2D HSQC and TROSY NMR spectra. Spectra of uniformly

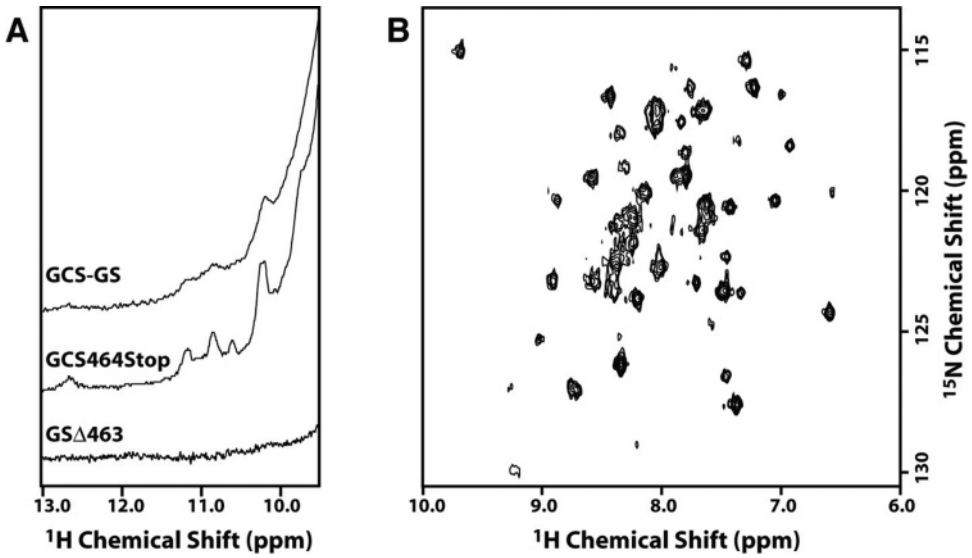

FIGURE 3: NMR spectra of γ-GCS-GS, GCS464Stop, and GSΔ463. Panel A: 1D ^{1}H NMR spectra of γ-GCS-GS (top), GCS464Stop (middle), and GSΔ463 (bottom). Panel B: 2D ^{1}H$-^{15}$N TROSY spectrum of [^{15}N]Leu-labeled GCS464Stop.

^{15}N-labeled and [^{15}N]Leu-labeled γ-GCS-GS contained dispersed signals consistent with a folded protein that were too weak to interpret, which we attribute to the long rotational correlation time of the intact dimeric enzyme and resulting line broadening. A TROSY spectrum obtained for [^{15}N]Leu-labeled GCS464Stop (Figure 3B) contains ~55 well-resolved peaks, approximately the number expected for this fragment, which contains 64 Leu residues. In contrast to the spectra of [^{15}N]γ-GCS-GS and [^{15}N]GCS464Stop, 2D spectra obtained for [^{15}N]GSΔ463 contained no resolved signals and only a very weak region of broad signal intensity that could be attributed to poorly folded protein (data not shown). Note that GSΔ463, even as the expected dimer, is in a M_r range where well-resolved peaks would be expected if the protein adopted a stable folded conformation. The 1D and ^{1}H$-^{15}$N 2D NMR spectra support the conclusion that both γ-GCS-GS and GCS464Stop are well-folded whereas GSΔ359, GSΔ440, and GSΔ463 are largely unfolded.

Determination of the Quaternary Structure of S. agalactiae γ-GCS-GS. The quaternary structure of full-length γ-GCS-GS and the most active γ-GCS domain, GCS464Stop, were determined by gel filtration (see Methods). Full-length γ-GCS-GS eluted with an apparent M_r of ~200 kDa, suggesting that the protein is a dimer of 88 kDa subunits (data not shown). This result, consistent with the recent report by B. Vergauwen et al. (*7*), differs from our earlier finding that γ-GCS-GS was a monomer (*5*), a result we now attribute to inadequate resolution of proteins on a smaller gel filtration column. The most active γ-GCS domain, GCS464Stop, eluted with a M_r of ~50 kDa, indicating that it is a monomer (i.e., the calculated M_r is 54 kDa) (data not shown).

Characterization of Site-Directed Mutants of S. agalactiae γ-GCS-GS. Histidine 144 of *S. agalactiae* γ-GCS-GS corresponds to H150 of *E. coli* γ-GCS, a residue that coordinates an essential Mg^{2+} ion and interacts with substrate glutamate (*18*). Since the H150A mutant of *E. coli* γ-GCS has <1% of WT activity (*25*), the *S. agalactiae* γ-GCS-GS H144A mutant was expressed and purified to near homogeneity. Isolated H144A γ-GCS-GS exhibited extremely low γ-GCS activity (~1% WT) (Table 3) but had GS activity somewhat higher than the WT enzyme (Table 4). Steady-state kinetic studies indicated that the K_m values for all γ-GCS substrates were markedly increased (6−10-fold) (Table 3). For the GS activity, K_m values for γ-GluCys, glycine, and ATP were essentially the same for H144A γ-GCS-GS as observed with WT γ-GCS-GS (Table 4).

Table 3: Comparison of K_m Values of γ-GCS Substrates and V_{max} Values for γ-GCS Activity among *S. agalactiae* WT γ-GCS-GS, H144A γ-GCS-GS, and K526A γ-GCS-GS

kinetic constant[a]	WT γ-GCS-GS[c]	H144A γ-GCS-GS	K526A γ-GCS-GS
K_m(L-glutamate) (mM)	22 ± 1	229 ± 36	24 ± 0.6
K_m(L-cysteine)	156 ± 9 μM	1.0 ± 0.2 mM	147 ± 5 μM
K_m(ATP)	64 ± 11 μM	622 ± 13 μM	69 ± 8 μM
V_{max}[b] (units/mg)	1290 ± 63	15.6 ± 1.7	1275 ± 44

[a] γ-GCS activity of γ-GCS-GS was assayed on the basis of ADP formation as described in Methods. Saturating levels of nonvaried substrates were used: 100 mM L-glutamate, 10 mM L-cysteine, 10 mM ATP, and 35 mM $MgCl_2$. Values shown are means ± SD of triplicate determinations. [b] V_{max} values shown are the means ± SD from all substrate studies. [c] Reference *5*.

As noted, residue alignments between the putative GS domain of *S. agalactiae* γ-GCS-GS and *E. coli* D-Ala, D-Ala ligase or GS are tentative and dependent on where one assumes the GS domain starts. Nonetheless, our structure-based alignment and the alignment proposed by B. Vergauwen et al. (*7*) show K526 aligning with a critical lysine residue present in both *E. coli* D-Ala, D-Ala ligase and *E. coli* GS; that lysine lies in a structurally important β-strand in both *E. coli* enzymes (*30*, *31*, *33*). The K526A γ-GCS-GS mutant was therefore constructed and purified to near homogeneity. As expected, K526A γ-GCS-GS retains full γ-GCS activity with no significant change in substrate K_m values (Table 3), but it exhibits very low GS activity (<0.5% WT) with modestly increased (~1.5-fold) substrate K_m values (Table 4). This result confirms that the GS activity resides in the C-terminus of γ-GCS-GS (*5*−*7*) and supports the general correctness of the GS domain alignments.

To elucidate the importance of residues in parts of the sequence possibly shared by the domains (i.e., residues 360−520), site-directed mutagenesis was used to mutate the three charged residues within that sequence that are conserved in

Table 4: Comparison of K_m Values of GS Substrates and V_{max} Values for GS Activity among *S. agalactiae* WT γ-GCS-GS, H144A γ-GCS-GS, K526A γ-GCS-GS, D448A γ-GCS-GS, K485A γ-GCS-GS, and K489A γ-GCS-GS

kinetic constant[a]	WT γ-GCS-GS[d]	H144A γ-GCS-GS	K526A γ-GCS-GS	D448A γ-GCS-GS	K485A γ-GCS-GS	K489A γ-GCS-GS
K_m(γ-GluCys) (mM)	5.9 ± 0.5	9.6 ± 0.3	7.5 ± 2.2	7.5 ± 1.5	ND[c]	31 ± 2
K_m(glycine) (mM)	6.3 ± 0.7	7.4 ± 0.6	11.8 ± 0.8	23.8 ± 0.4	ND[c]	28 ± 2
K_m(ATP)	420 ± 49 μM	447 ± 43 μM	624 ± 18 μM	4.9 ± 0.2 mM	ND[c]	13.4 ± 0.8 mM
V_{max}[b] (units/mg)	2383 ± 66	2958 ± 58	9.9 ± 2.3	134.3 ± 0.9	2.5 ± 0.4	89 ± 2

[a] GS activity of γ-GCS-GS was assayed on the basis of ADP formation as described in Methods. Saturating levels of nonvaried substrates were used: 25 mM γ-GluCys, 25 mM glycine, 10 mM ATP, and 35 mM $MgCl_2$. Values shown are means ± SD of triplicate determinations. [b] V_{max} values shown are the means ± SD from all substrate studies. [c] K_m values were not obtained due to instability of the GS activity for K485A γ-GCS-GS. [d] Reference *5*.

Table 5: Comparison of K_m Values of γ-GCS and GS Substrates, V_{max} Values for γ-GCS and GS Activities, and K_i Values of GSH Inhibition among Expressed *S. agalactiae* γ-GCS-GS Chimeric Enzymes and WT γ-GCS-GS Enzymes

kinetic constant[a]	WT *S. agalactiae* γ-GCS-GS[c]	*S. agalactiae* γ-GCS-GS−*E. faecalis* γ-GCS-GS loop	WT *E. faecalis* γ-GCS-GS	*S. agalactiae* γ-GCS-GS−*P. multocida* γ-GCS-GS loop	WT *P. multocida* γ-GCS-GS[e]
K_m(L-Glu) (mM)	22 ± 1	90 ± 1	79 ± 14	24 ± 2	5.3 ± 0.3
K_m(L-Cys) (μM)	156 ± 9	293 ± 35	192 ± 14	258 ± 10	220 ± 32
K_m(ATP) (μM)	64 ± 11	44 ± 3	2300 ± 100	86 ± 8	250 ± 24
K_i(GSH) (mM)	141 ± 23[d]	>200	25.1 ± 0.8	168 ± 19	13.6
γ-GCS V_{max}[b] (units/mg)	1290 ± 63	1109 ± 9	240 ± 11	1080 ± 32	1006
K_m(γ-GluCys) (mM)	6.3 ± 0.7	11.5 ± 2.1	5.0 ± 0.5	9.4 ± 0.2	0.09 ± 0.009
K_m(glycine) (mM)	5.9 ± 0.5	4.3 ± 0.2	4.3 ± 0.1	3.4 ± 0.4	81 ± 12
K_m(ATP) (μM)	420 ± 50	471 ± 40	179 ± 5	509 ± 28	530 ± 65
GS V_{max}[b] (units/mg)	2383 ± 66	1750 ± 24	2300 ± 42	2002 ± 50	1254

[a] γ-GCS and GS activities of γ-GCS-GS were assayed on the basis of ADP formation as described in Methods. Values shown are either averages of duplicate measurements or means ± SD for triplicate determinations. Saturating levels of nonvaried substrates were used: 100 mM L-glutamate, 10 mM L-cysteine, 25 mM γ-GluCys, 25 mM glycine, 10 mM ATP, and 35 mM $MgCl_2$. [b] V_{max} values shown are the means ± SD from all substrate studies. [c] Reference *5*. [d] This work. [e] Reference *7*.

all 19 known γ-GCS-GS sequences. Thus, we constructed, expressed, and purified the D448A, K485A, and K489A mutants of *S. agalactiae* γ-GCS-GS as His-tagged fusion proteins and assayed them for both γ-GCS and GS activity. All three mutants exhibited uniformly low levels of GS activity (i.e., <10% WT GS activity) and in the case of D448A and K489A significantly increased GS domain substrate K_m values, especially for glycine and ATP (Table 4). The GS activity of the K485A mutant was very low and decreased within hours of isolation; substrate K_m values were therefore not determined. Although each of the three mutants involved residues in a part of the sequence implicated as important in γ-GCS domain catalysis or susceptibility to GSH inhibition, all retained full γ-GCS activity with no significant change in substrate K_m values. As with WT γ-GCS-GS, the γ-GCS activity was resistant to inhibition by GSH (K_i = 288, 173, 300, and 167 mM for D448A, K485A, K489A, and K526A, respectively). That finding suggests that none of the mutations caused major structural reorientation of the affected sequence.

Expression and Characterization of E. faecalis γ-GCS-GS. E. faecalis γ-GCS-GS was expressed and purified to near homogeneity as described in Methods. Specific activities for γ-GCS and GS were 240 and 2300 units/mg, respectively, and substrate K_m values were found in some cases to be distinct from *S.* agalactiae γ-GCS-GS (Table 5). Note in particular the much higher K_m values for glutamate (90 vs 22 mM) and ATP (2300 vs 64 μM) for the γ-GCS activity. In contrast to *S. agalactiae* γ-GCS-GS, *E. faecalis* γ-GCS-GS is significantly inhibited by GSH (K_i = 25.1 ± 0.8 mM), which bound competitively with glutamate (Table 5).

```
S. agalactiae γ-GCS-GS    246 KSGQLIAEKEFYS 259
P. multocida γ-GCS-GS     251 STGKLIAEKEFYS 263
E. faecalis γ-GCS-GS      251 ENGLLSEEKEFYA 263
E. coli γ-GCS             287 NSNVLQIENELYA 301
```

FIGURE 4: Alignment of a central flexible loop (β8−β9 loop in PDB codes 1V4G and 1VA6) of *E. coli* γ-GCS and putative flexible loops found in *S. agalactiae* γ-GCS-GS, *P. multocida* γ-GCS-GS, and *E. faecalis* γ-GCS-GS. Identical residues are highlighted in yellow. The loops of both *S. agalactiae* γ-GCS-GS and *P. multocida* γ-GCS-GS share 31% identity with *E. coli* γ-GCS and 77% identity with each other, while the loop of *E. faecalis* γ-GCS-GS shares 38% identity with the loop from *E. coli* γ-GCS and only 54% identity to the loop from either *S. agalactiae* γ-GCS-GS or *P. multocida* γ-GCS-GS.

Characterization of Chimeric γ-GCS-GS Enzymes. To elucidate the importance of a central flexible loop implicated as critical in GSH inhibition of *E. coli* γ-GCS (*18*) (see Discussion), chimeric enzymes were constructed in which the putative flexible loop (shown in pink in Figure 1C) of *S. agalactiae* γ-GCS-GS was altered to that present in either *P. multocida* or *E. faecalis* γ-GCS-GS (see Methods and Figure 4). Glutathione is reportedly a noncompetitive inhibitor of *P. multocida* γ-GCS-GS (*7*) and is, as noted, a competitive inhibitor of *E. faecalis* γ-GCS-GS (this work) as well as all native monofunctional γ-GCS enzymes examined to date. Chimeric enzymes were characterized with respect to both γ-GCS and GS activity, as well as γ-GCS activity inhibition by GSH (Table 5). Both chimeras exhibited substantial γ-GCS and GS activity with specific activities under saturating substrate conditions at least 40% of WT *S. agalactiae* γ-GCS-GS (Table 5). Substrate affinities for the γ-GCS domain were generally characteristic of *S. agalactiae* γ-GCS-GS and unlike either of the flexible loop donors (e.g.,

the much higher ATP K_m values of *E. faecalis* and *P. multocida* were not replicated in the chimeras). The exception was that the construct containing the *E. faecalis* flexible loop exhibited a very high glutamate K_m (~90 mM) that was similar to *E. faecalis* γ-GCS-GS (~79 mM) and significantly higher than native *S. agalactiae* γ-GCS-GS (~22 mM). Notably, GSH inhibition of the chimeras was very weak, mimicking that seen with *S. agalactiae* γ-GCS-GS rather than the more potent GSH inhibition observed in the flexible loop donor enzymes. The flexible loop chimeras would be expected to have unchanged substrate affinities for the unaltered GS domain, and in general, that was the case although the K_m for ATP was modestly increased in the chimera with a *P. multocida* loop.

DISCUSSION

Glutathione synthesis has been characterized in numerous eukaryotic (*27*, *29*, *34*−*41*) and Gram-negative prokaryotic (*25*, *28*, *42*) organisms. In these species, GSH synthesis is catalyzed by the sequential action of distinct enzymes, γ-GCS and GS. In contrast, GSH synthesis in three Gram-positive bacteria, *S. agalactiae* (*5*), *L. monocytogenes* (*6*), and *E. faecalis* (this work), and one Gram-negative bacterium, *P. multocida* (*7*), is catalyzed by a single bifunctional enzyme, γ-GCS-GS, which is the product of a single gene, *gshAB*. The genomes of at least 15 other, mostly Gram-positive bacteria contain a homologous gene, and those bacteria may also rely on γ-GCS-GS for GSH synthesis (*5*, *6*).[3]

Homology with *E. coli* γ-GCS strongly suggested that the γ-GCS active site of γ-GCS-GS was in the N-terminal portion of the enzyme, a view supported by sequence alignments (refs *5*−*7* and present work) but no previous experimental work. Sequence alignments provided little help in establishing the extent to which the putative γ-GCS domain and C-terminal GS domain overlap, interact, or are interdependent. Those questions were addressed in the present studies.

As expected, expression of N-terminal fragments of *S. agalactiae* γ-GCS-GS resulted in proteins with γ-GCS but not GS activity. Contrary to our initial hypothesis, but supported by a recently published alignment for *P. monocytogenes* γ-GCS-GS (*7*), the GCS464Stop protein had the greatest activity of several constructs made and thus best represents the γ-GCS domain (Figure 1C). Consistent with that conclusion, the activity of GCS464Stop (163 units/nmol) is ~84% of that we observe for *E. coli* γ-GCS [195 units/nmol; 3353 units/mg (*28*)], indicating that the active sites are capable of comparable catalytic efficiency (k_{cat}). Similarity of the k_{cat} values is, in turn, consistent with the fact that all residues known to be important in *E. coli* γ-GCS are identical or conservatively replaced in the modeled γ-GCS active site of *S. agalactiae* γ-GCS-GS (Figure 1A). That GCS464Stop represents the minimal core γ-GCS domain is supported by the finding that GCS441Stop, which is just 23 amino acids shorter, has a much lower specific activity (9 units/nmol). Although the deleted amino acids include no known key residues, it is likely that deletion of the 442−464 sequence affects the conformation of other residues more proximal to the active site. Supporting that view, the K_m for L-glutamate increased 3-fold in GCS441Stop relative to the other constructs and WT γ-GCS-GS.

Putative γ-GCS domain constructs longer than 464 amino acids had diminished activity but nearly unaltered substrate K_m values. Although we are unable to model the C-terminal extensions due to low sequence homology, the additional sequence in GCS494Stop appears to adopt a conformation similar to that in the native enzyme since the observed molar specific activity and substrate K_m values are close to WT values. The two constructs longer than 494 amino acids (i.e., GCS508Stop and GCS521Stop) had less than WT activity, suggesting their structures deviated from native enzyme in a manner that modestly reduced k_{cat} without significantly affecting K_m values. However, deviation from native structure is apparently small because both GCS508Stop and GCS521Stop remarkably recapitulate the resistance to GSH inhibition that is seen in WT γ-GCS-GS but lost in GCS464Stop and GCS494Stop.

The finding that the presence or absence of a short 13 amino acid sequence (i.e., residues 495−508) modulates GSH inhibition is of considerable interest. In mammals and *E. coli*, feedback inhibition of γ-GCS by GSH is an important physiological regulator of GSH synthesis, and apparent K_i values are in the range of typical intracellular GSH levels (i.e., 1−5 mM) (*27*, *44*). In contrast, *S. agalactiae* γ-GCS-GS is very weakly inhibited by GSH (K_i ~ 140 mM), and the bacteria are consequently able to maintain exceptionally high GSH concentrations (>75 mM) (*5*). As noted, resistance to GSH inhibition is lost in GCS464Stop and GCS494Stop, where the K_i values for GSH (13 and 18 mM, respectively) are only 56% and 83%, respectively, of the K_m values for glutamate, the substrate with which GSH competes for binding (Table 2). That is a relatively stronger inhibition than is seen even with *E. coli* γ-GCS, where K_i (GSH) is severalfold higher than K_m (Glu) when measured under conditions comparable to those used here (i.e., cysteine site substrate at 10-fold its K_m) (B. S. Kelly and O. W. Griffith, unpublished results). Our results thus suggest that residues between 494 and 508, either directly or through interactions with other regions of the sequence, induce a conformation of the γ-GCS domain to which GSH cannot easily bind. Because γ-GluCys is an effective inhibitor of WT γ-GCS-GS and both long and short truncation mutants (Table 1), our results indicate further that it is the glycine residue of GSH that is uniquely not accommodated by the GCS508Stop, GCS520Stop, and WT γ-GCS-GS active sites.

To date, the structural basis for GSH inhibition of γ-GCS has not been directly established for any species. The nearly universal observation that GSH binds competitively with glutamate[4] indicates that GSH binds in the active site (i.e.,

[3] It remains to be determined if all *gshAB*-containing bacteria actually make GSH. *Streptococcus mutans* contains a putative *gshAB* quite similar to that of *S. agalactiae*, but *S. mutans* reportedly takes up GSH from its medium and does not synthesize the tripeptide (*4*), an observation we have confirmed under a limited number of growth conditions (B. E. Janowiak and O. W. Griffith, unpublished results). It is thus not certain that all *gshAB*-containing bacteria express active γ-GCS-GS. Initial studies with *S. mutans* γ-GCS-GS expressed in *E. coli* show the enzyme to be active and inhibited by GSH, although large-scale purification and full characterization have been prevented thus far by inclusion body formation (B. E. Janowiak, M. A. Hayward, and O. W. Griffith, unpublished results).

[4] Previously documented exceptions to competitive inhibition are the catalytic heavy subunit of rat γ-GCS (*43*) and *P. multocida* γ-GCS-GS (*7*).

nonallosterically), but the fact that cysteinylglycine neither replaces cysteine as a substrate nor inhibits has made it difficult to understand how the cysteinylglycine portion of GSH is accommodated in the active site. New insight into this problem was recently provided by T. Hibi et al., who obtained crystal structures of *E. coli* γ-GCS with and without a transition state analogue of γ-GluCys bound (*18*). They showed that *E. coli* γ-GCS exists in two conformations determined by the position of a centrally located flexible loop: a closed conformation, which is favored by cysteine binding and does not have space for the glycine moiety of GSH, and an open conformation in which GSH appears to be able to fit in the otherwise unoccupied glutamate and cysteine binding sites with its glycine moiety extending into a open cavity beyond the cysteine site (*18*). Our results suggest two possible explanations for the weak GSH inhibition seen in WT γ-GCS-GS: (i) the 495−508 sequence itself projects into the cavity that would otherwise accommodate the glycine moiety of GSH or (ii) the presence of the 495−508 sequence causes the flexible loop to adopt a partially closed position that prevents the glycine moiety of GSH from binding. To distinguish these possibilities, we constructed chimeras of *S. agalactiae* γ-GCS-GS in which the flexible loop was replaced by loops from the *E. faecalis* or *P. multocida* γ-GCS-GS isoforms, both of which are subject to GSH inhibition. Inhibition by GSH remained weak in both chimeras, suggesting it is not the sequence of the flexible loop alone that prevents or allows GSH binding. Additional studies will be needed to explore the possibility that more complex interactions between residues on the loop, residues in the 495−508 region, and perhaps residues in the putative glycine-accommodating cavity account the differences in GSH inhibition.

Whereas the various N-terminal γ-GCS domain constructs of *S. agalactiae* γ-GCS-GS are well folded and exhibit WT levels of activity, expressed proteins corresponding to the putative C-terminal GS domain had little GS activity. Activity was not increased by removing the N-terminal His_8 tag or by addition of γ-GCS domain proteins corresponding to the sequence deleted in making the GS domain constructs. Low GS activity is also not explained by the need to include additional N-terminal sequence. The longest GS domain constructs, GSΔ293 and GSΔ359, were large enough to include sequence that clearly contributes to γ-GCS activity and is part of that domain, and yet those N-terminally extended species still had little GS activity. Notwithstanding the low activity observed, it is clear that the C-terminal sequence accounts for GS activity in WT γ-GCS-GS since truncation at residue 466 eliminated GSH but not γ-GluCys synthesis in *L. monocytogenes* γ-GCS-GS (*6*) and mutation of a well-conserved lysine residue at position 526 (K526A) in *S. agalactiae* γ-GCS-GS nearly eliminates GS activity while having essentially no effect on γ-GCS activity (present studies). Absence of significant activity in the expressed GS domains thus appears to be due to poor folding. Both CD and NMR studies of the GS domains confirm that view, showing little evidence of secondary or tertiary structure.

Near absence of GS activity in the K526A mutant establishes that the GS domain extends at least that far toward the N-terminus. Additional site-directed mutants were designed as described in Methods to establish more precisely the N-terminal limit of the GS domain. Single mutations in

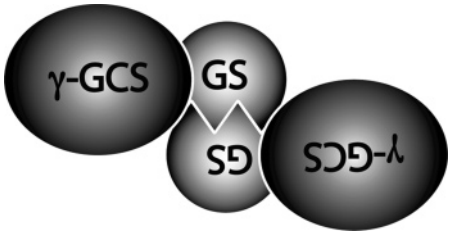

FIGURE 5: Model of domain interactions for γ-GCS-GS. Schematic depicting γ-GCS-GS comprised of independently folding, globular γ-GCS domain monomers and a closely interfacing GS domain dimer that is structurally dependent on the γ-GCS domains.

γ-GCS-GS at D448, K485, and K489 resulted in proteins with WT γ-GCS activity and little susceptibility to GSH inhibition, but with <8% of WT GS activity. Note that D448 is in the 441−464 sequence which, if deleted, reduces γ-GCS activity by 91%. It is thus apparent that the domains are codependent on some of the same sequence. These findings suggest further that K485 and K526 have structural rather than substrate binding roles since K485A γ-GCS-GS exhibited highly unstable GS activity and K526A, which, as noted, maps to a structurally important β-sheet, showed greatly reduced GS activity without significant changes in substrate K_m values. Mutation of D448 and K489, on the other hand, increased the K_m values for ATP and glycine by 4−30-fold, suggesting that they participate in the active site or at least indirectly affect residues in the GS active site. Taken together, our results suggest that residues between ∼441 and ∼520 serve multiple functions. Those between 441 and 464 are needed for full γ-GCS activity, those between 495 and 508 control GSH inhibition in a manner not yet fully elucidated, and residues as early as 448 and 489 affect binding of substrates to the GS active site. These conclusions differ from those reached on the basis of alignment studies with *P. monocytogenes* γ-GCS-GS, which suggested that the γ-GCS domain (1−462) and GS domain (480−757) are distinct structures and connected by an 18 amino acid linker (*7*).

Although six GS domain constructs were made and tested, none showed significant activity, and only the longest had evidence of secondary structure (see Figure 2). While other explanations are possible, we think it most likely that proper folding of the GS domain requires a covalently attached γ-GCS domain. Thus, our results argue strongly that the γ-GCS-GS structure is comprised of an independently folding, globular γ-GCS domain, similar to that modeled in Figure 1C, and a closely interfacing GS domain that relies on part of the γ-GCS domain surface for its structural integrity and folding (Figure 5). Dimerization through the GS domain is supported by the observations that full-length *S. agalactiae* γ-GCS-GS is a dimer (this work),[2] that GCS464Stop is a monomer (this work), that *E. coli* γ-GCS is a monomer (*18*), and that plausible evolutionary precursors of the GS domain are multimers [e.g., *E. coli* D-Ala, D-Ala ligase is a homodimer (*30*) and *E. coli* GS is a homotetramer (*31*)].

The model in Figure 5 finds support in the presumed ancestry of γ-GCS-GS. As discussed elsewhere (*5*, *6*), it is believed that γ-GCS-GS arose in a primitive bacteria that initially contained only a monomeric γ-GCS. That species maintained its ability to independently fold and exhibit activity but became fused through its C-terminus to an ATP-

grasp domain, presumably by duplication of the gene for an existing ATP-grasp domain protein. Interestingly, B. Vergauwen et al. identified in the *Clostridium acetobutylicum* genome sequences with significant homology to the γ-GCS and GS domains of γ-GCS-GS separated by about 80 base pairs (*7*); that arrangement may represent a transitional form existing before fusion. In any case, we hypothesize that further evolution of the fused C-terminal ATP-grasp domain to acquire GS activity occurred after fusion and therefore in proximity to the γ-GCS domain. Consistent with the observations reported herein, the resulting GS domain would then likely depend on parts of the properly folded γ-GCS domain for its own folding, substrate binding, and catalytic activity.

S. agalactiae γ-GCS-GS differs markedly from the γ-GCS-GS of other bacteria in being resistant to inhibition by GSH. Consistent with that resistance, *S. agalactiae* maintains levels of GSH [~75 mM (*5*)] that are much higher than those in *E. coli* [~5 mM (*45*)], *E. faecalis* [~15 mM (B. E. Janowiak and O. W. Griffith, unpublished results)], *P. multocida* [(~3−20 mM (*7*)], or mammalian cells [~1−10 mM (*46*)]. Such high levels may be important to the survival of *S. agalactiae* since the bacterium is both catalase-deficient and has no obvious GSH peroxidase in its genome. We hypothesize that *S. agalactiae* may rely more than other cells on the direct chemical reaction of GSH with oxidants, a process that obeys the law of mass action.

The present studies identified several additional differences among γ-GCS-GS isoforms. There are, for example, marked differences with respect to substrate K_m values and the relative activities of the γ-GCS and GS domains [e.g., for the γ-GCS activity, K_m(Glu) ranges from 5 to 79 mM and K_m(ATP) ranges from 64 to 2300 μM; for the GS activity, K_m(γ-GluCys) ranges from 0.09 to 6 mM and K_m(Gly) ranges from 4 to 81 mM]. Specific activities for enzymes reportedly purified to homogeneity range from 16 to 1300 units/mg for the γ-GCS activity and from 15 to 2400 units/mg for the GS activity (refs *5*−*7* and present work). B. Vergauwen et al. report that the *P. monocytogenes* enzyme exhibits half-the-sites reactivity, cooperative inhibition of the γ-GCS activity by glycine (which has a remarkably high K_m of 81 mM), and noncompetitive inhibition by GSH. None of those effects are seen with the *S. agalactiae* isoform. Although the differences can be accounted for by the relatively modest sequence identity (~45%) and similarity (~65%) among the isoforms listed, it is notable that the differences potentially offer very different mechanisms through which intracellular GSH levels may be controlled (e.g., substrate availability where K_m's are high, presence or absence of GSH inhibition which can be competitive or noncompetitive with glutamate, interdomain interaction through half-the-sites reactivity). It will be of considerable interest to determine the structural and kinetic basis of these regulatory mechanisms and to correlate those findings with the bacteria-specific biological role of the enzymes and GSH.

ACKNOWLEDGMENT

We thank Davin Jensen for technical assistance.

REFERENCES

1. Fahey, R. C., Newton, G. L., Arrick, B., Overdank-Bogart, T., and Aley, S. B. (1984) *Entamoeba histolytica*: a eukaryote without glutathione metabolism, *Science 224*, 70−72.
2. Newton, G. L., Arnold, K., Price, M. S., Sherrill, C., Delcardayre, S. B., Aharonowitz, Y., Cohen, G., Davies, J., Fahey, R. C., and Davis, C. (1996) Distribution of thiols in microorganisms: mycothiol is a major thiol in most actinomycetes, *J. Bacteriol. 178*, 1990−1995.
3. Fahey, R. C., Brown, W. C., Adams, W. B., and Worsham, M. B. (1978) Occurrence of glutathione in bacteria, *J. Bacteriol. 133*, 1126−1129.
4. Sherrill, C., and Fahey, R. C. (1998) Import and metabolism of glutathione by *Streptococcus mutans*, *J. Bacteriol. 180*, 1454−1459.
5. Janowiak, B. E., and Griffith, O. W. (2005) Glutathione synthesis in *Streptococcus agalactiae*. One protein accounts for gamma-glutamylcysteine synthetase and glutathione synthetase activities, *J. Biol. Chem. 280*, 11829−39.
6. Gopal, S., Borovok, I., Ofer, A., Yanku, M., Gohen, G., Goebel, W., Kreft, J., Aharonowitz, Y. (2005) A multidomain fusion protein in *Listeria monocytogenes* catalyzes the two primary activites for glutathione biosynthesis, *J. Bacteriol. 187*, 3839−3847.
7. Vergauwen, B., De Vos, D., and Beeumen, J. J. (2006) Characterization of the bifunctional γ-glutamate-cysteine ligase-glutathione synthetase (GshF) of *Pasteurella multocida*, *J. Biol. Chem. 281*, 4380−4394.
8. Strumeyer, D., and Bloch, K. (1962) gamma-L-glutamyl-L-cysteine from glutathione, *Biochem. Prep. 9*, 52−55.
9. Dougherty, W. G., Cary, S. M., and Parks, T. D. (1989) Molecular genetic analysis of a plant virus polyprotein cleavage site: a model, *Virology 171*, 356−364.
10. Waltner, J. K., Peterson, F. C., Lytle, B. L., and Volkman, B. F. (2005) Structure of the B3 domain from *Arabidopsis thaliana* protein At1g16640, *Protein Sci. 14*, 2478−2483.
11. Paulsen, I. T., Banerjei, L., Myers, G. S. A., Nelson, K. E., Seshadri, R., Read, T. D., Fouts, D. E., Eisen, J. A., Gill, S. R., Heidelberg, J. F., Tettelin, H., Dodson, R. J., Umayam, L., Brinkac, L., Beanan, M., Daugherty, S., DeBoy, R. T., Durkin, S., Kolonay, J., Madupu, R., Nelson, W., Vamathevan, J., Tran, B., Upton, J., Hansen, T., Shetty, J., Khouri, H., Utterback, T., Radune, D., Ketchum, K. A., Dougherty, B. A., Fraser, C. M. (2003) Role of mobile DNA in the evolution of vancomycin-resistant *Enterococcus faecalis*, *Science 299*, 2071−2074.
12. Weber, D. J., Gittis, A. G., Mullen, G. P., Abeygunawardana, C., Lattman, E. E., and Mildvan, A. S. (1992) NMR docking of a substrate into the X-ray structure of staphylococcal nuclease, *Proteins 13*, 275−287.
13. Bradford, M. M. (1976) A rapid and sensitive method for the quantitation of microgram quantities of protein utilizing the principle of protein-dye binding, *Anal. Biochem. 72*, 248−254.
14. Pace, C. N., Vajdos, F., Fee, L., Grimsley, G., and Gray, T. (1995) How to measure and predict the molar absorption coefficient of a protein, *Protein Sci. 4*, 2411−2423.
15. Mori, S., Abeygunawardana, C., Johnson, M. O., and van Zijl, P. C. (1995) Improved sensitivity of HSQC spectra of exchanging protons at short interscan delays using a new fast HSQC (FHSQC) detection scheme that avoids water saturation, *J. Magn. Reson. B 108*, 94−98 [erratum: (1996) *J. Magn. Reson. B 110*, 321].
16. Pervushin, K., Riek, R., Wider, G., and Wuthrich, K. (1997) Attenuated T2 relaxation by mutual cancellation of dipole−dipole coupling and chemical shift anisotropy indicates an avenue to NMR structures of very large biological macromolecules in solution, *Proc. Natl. Acad. Sci. U.S.A. 94*, 12366−12371.
17. Notredame, C., Higgins, D. G., and Heringa, J. (2000) T-coffee: a novel method for fast and accurate multiple sequence alignment, *J. Mol. Biol. 302*, 205−217.
18. Hibi, T., Nii, H., Nakatsu, T., Kimura, A., Kato, H., Hiratake, J., and Oda, J. (2004) Crystal structure of gamma-glutamylcysteine synthetase: insights into the mechanism of catalysis by a key enzyme for glutathione homeostasis, *Proc. Natl. Acad. Sci. U.S.A. 101*, 15052−15057.
19. Eswar, N., John, B., Mirkovic, N., Fiser, A., Ilyin, V. A., Pieper, U., Stuart, A. C., Marti-Renom, M. A., Madhusudhan, M. S., Yerkovich, B., and Sali, A. (2003) Tools for comparative protein structure modeling and analysis, *Nucleic Acids Res. 31*, 3375−3380.
20. Fiser, A., and Sali, A. (2003) Modeller: generation and refinement of homology-based protein structure models, *Methods Enzymol. 374*, 461−491.

21. Laskowski, R. A., MacArthur, M. W., Moss, D. S., and Thornton, J. M. (1993) PROCHECK: a program to check the stereochemical quality of protein structures, *J. Appl. Crystallogr. 26*, 283−291.
22. Pontius, J., Richelle, J., and Wodak, S. J. (1996) Deviations from standard atomic volumes as a quality measure for protein crystal structures, *J. Mol. Biol. 264*, 121−136.
23. Melo, F., and Feytmans, E. (1998) Assessing protein structures with a nonlocal atomic interaction energy, *J. Mol. Biol. 277*, 1141−1152.
24. Colovos, C., and Yeates, T. O. (1993) Verification of protein structures: Patterns of nonbonded atomic interactions, *Protein Sci. 2*, 1511−1519.
25. Inoue, Y., Iba, Y., Yano, H., Murata, K., and Kimura, A. (1993) Functional analysis of the gamma-glutamylcysteine synthetase of *Escherichia coli* B: effect of substitution of His-150 to Ala, *Appl. Microbiol. Biotechnol. 38*, 473−477.
26. Thompson, J. D., Higgins, D. G., and Gibson, T. J. (1994) CLUSTAL W: improving the sensitivity of progressive multiple sequence alignment through sequence weighting, position-specific gap penalties and weight matrix choice, *Nucleic Acids Res. 22*, 4673−4680.
27. Griffith, O. W., and Mulcahy, R. T. (1999) The enzymes of glutathione synthesis: gamma-glutamylcysteine synthetase, *Adv. Enzymol. Relat. Subj. Biochem. 73*, 209−267.
28. Kelly, B. S., Antholine, W. E., and Griffith, O. W. (2002) *Escherichia coli* gamma-glutamylcysteine synthetase. Two active site metal ions affect substrate and inhibitor binding, *J. Biol. Chem. 277*, 50−58.
29. Misra, I., and Griffith, O. W. (1998) Expression and purification of human gamma-glutamylcysteine synthetase, *Protein Expression Purif. 13*, 268−276.
30. Fan, C., Moews, P. C., Walsh, C. T., and Knox, J. R. (1994) Vancomycin resistance: structure of D-alanine:D-alanine ligase at 2.3 Å resolution, *Science 266*, 439−443.
31. Hara, T., Kato, H., Katsube, Y., and Oda, J. (1996) A pseudo-michaelis quaternary complex in the reverse reaction of a ligase: structure of *Escherichia coli* B glutathione synthetase complexed with ADP, glutathione, and sulfate at 2.0 Å resolution, *Biochemistry 35*, 11967−11974.
32. Fan, C., Moews, P. C., Shi, Y., Walsh, C. T., and Knox, J. R. (1995) A common fold for peptide synthetases cleaving ATP to ADP: glutathione synthetase and D-alanine:D-alanine ligase of *Escherichia coli*, *Proc. Natl. Acad. Sci. U.S.A. 92*, 1172−1176.
33. Shi, Y., and Walsh, C. T. (1995) Active site mapping of *Escherichia coli* D-Ala-D-Ala ligase by structure-based mutagenesis, *Biochemistry 34*, 2768−2776.
34. Tu, Z., and Anders, M. W. (1998) Expression and characterization of human glutamate-cysteine ligase, *Arch. Biochem. Biophys. 354*, 247−254.
35. Sekura, R., and Meister, A. (1977) gamma-Glutamylcysteine synthetase. Further purification, "half of the sites" reactivity, subunits, and specificity, *J. Biol. Chem. 252*, 2599−2605.
36. May, M. J., and Leaver, C. J. (1994) *Arabidopsis thaliana* gamma-glutamylcysteine synthetase is structurally unrelated to mammalian, yeast, and *Escherichia coli* homologs, *Proc. Natl. Acad. Sci. U.S.A. 91*, 10059−10063.
37. Lueder, D. V., and Phillips, M. A. (1996) Characterization of *Trypanosoma brucei* gamma-glutamylcysteine synthetase, an essential enzyme in the biosynthesis of trypanothione (diglutathionylspermidine), *J. Biol. Chem. 271*, 17485−17490.
38. Hussein, A. S., and Walter, R. D. (1995) Purification and characterization of gamma-glutamylcysteine synthetase from Ascaris suum, *Mol. Biochem. Parasitol. 72*, 57−64.
39. Brekken, D. L., and Phillips, M. A. (1998) *Trypanosoma brucei* gamma-glutamylcysteine synthetase. Characterization of the kinetic mechanism and the role of Cys-319 in cystamine inactivation, *J. Biol. Chem. 273*, 26317−26322.
40. Jez, J. M., Cahoon, R. E., and Chen, S. (2004) *Arabidopsis thaliana* glutamate-cysteine ligase: functional properties, kinetic mechanism, and regulation of activity, *J. Biol. Chem. 279*, 33463−33470.
41. Phlippen, N., Hoffmann, K., Fischer, R., Wolf, K., and Zimmermann, M. (2003) The glutathione synthetase of *Schizosaccharomyces pombe* is synthesized as a homodimer but retains full activity when present as a heterotetramer, *J. Biol. Chem. 278*, 40152−40161.
42. Huang, C. S., Moore, W. R., and Meister, A. (1988) On the active site thiol of gamma-glutamylcysteine synthetase: relationships to catalysis, inhibition, and regulation, *Proc. Natl. Acad. Sci. U.S.A. 85*, 2464−2468.
43. Huang, C.-S., Chang, L.-S., Anderson, M. E., and Meister, A. (1993) Catalytic and regulatory properties of the heavy subunit of rat kidney γ-glutamylcysteine synthetase, *J. Biol. Chem. 268*, 19675−19680.
44. Meister, A., and Anderson, M. E. (1983) Glutathione, *Annu. Rev. Biochem. 52*, 711−760.
45. Cayley, S., Lewis, B. A., Guttman, H. J., and Record, M. T., Jr. (1991) Characterization of the cytoplasm of *Escherichia coli* K-12 as a function of external osmolarity. Implications for protein-DNA interactions in vivo, *J. Mol. Biol. 222*, 281−300.
46. Griffith, O. W. (1980) Determination of glutathione and glutathione disulfide using glutathione reductase and 2-vinylpyridine, *Anal. Biochem. 106*, 207−212.

BI052483V